Chinese Chemical Letters 34 (2023) 107238

Contents lists available at ScienceDirect

Chinese Chemical Letters

journal homepage: www.elsevier.com/locate/cclet

DL-Serine covalently modified multinuclear lanthanide-implanted arsenotungstates with fast photochromism

Kangting Zheng, Bingxue Niu, Cunmeng Lin, Yizhen Song, Pengtao Ma*, Jingping Wang, Jingyang Niu*

Henan Key Laboratory of Polyoxometalate Chemistry, College of Chemistry and Chemical Engineering, Henan University, Kaifeng 475004, China

ARTICLE INFO

Article history:
Received 30 December 2021
Revised 8 February 2022
Accepted 17 February 2022
Available online 20 February 2022

Keywords:
Polyoxometalate
Arsenotungstate
Carboxylate covalently modified
Lanthanide
Photochromism

ABSTRACT

A series of DL-serine covalently modified multinuclear lanthanide implanted arsenotungstates $K_2[\{Ln(H_2O)_7\}_2\{As_4W_{44}O_{137}(OH)_{18}(H_2O)_2(DL\text{-}Ser)_2\}\{Ln_2(H_2O)_5(DL\text{-}Ser)\}_2]\cdot 65H_2O$ (DL-Ser = DL-serine, Ln = La (**1**), Ce (**2**), Pr (**3**)) are obtained. Crystal structure analysis shows that these compounds are isomorphic and contain the basic $[\{As_4W_{44}O_{137}(OH)_{18}(H_2O)_2(DL\text{-}Ser)_2\}\{Ln_2(H_2O)_5(DL\text{-}Ser)\}_2]^{8-}$ polyoxoanion constituted by two $\{As_2W_{19}O_{59}(OH)_8(H_2O)\}^{6-}$ subunits, a $[W_6O_{23}(OH)_2(DL\text{-}Ser)_2]^{14-}$ fragment, and two embedded $[Ln_2(H_2O)_5(DL\text{-}Ser)]^{5+}$ groups, which further build into one dimensional linear chainlike structure *via* two peripheral Ln^{3+} ions. Most remarkably, these compounds exhibit rapid photochromic behaviors, which changed color quickly from white (**1**), yellow (**2**), green (**3**) to blue (**1**), brown (**2**) and glaucous (**3**) in ten minutes under UV irradiation, and that the colors gradually recovered in the dark for approximately 22 h.

The organic-inorganic hybrid polyoxometalates (POMs) are a class of molecular-based nanomaterials with required morphologies and functionalities, which show excellent physical and chemical properties [1–4]. Among them, carboxylate covalently modified POM derivatives have received more and more attention in recent years owing to the performance advantages of both organic components and POMs groups, which have broad application prospects in the fields of catalysis, optoelectronic functional material, owing to excellent photoelectric and photochromic properties [5,6]. Carboxylates can be considered to be involved in the backbone of POMs as the following characteristics: (1) multiple coordination modes of the carboxyl, where a carboxylate group can coordinate to one or two metal centers; (2) diverse types, mono-, di- or multiple carboxyl group in one carboxylate ligand; (3) as flexible aliphatic ligand or rigid aromatic carboxylate ligand; (4) as a template agent for modulating the structure. More importantly, the carboxylate ligand covalently binding to the POM cluster significantly disperses the surface electronegativity of the polyoxoanion skeleton, and gives rise to strong d-pπ interactions for improving the structural stability and photoreactivity of the POMs [1,7].

At present, the carboxylate covalently modified POM derivatives have mostly focused on polyoxovanadates and polyoxomolybdates [7,8]. Some impressive examples of carboxylate covalently modified polyoxovanadates have been made such as nano-sized cage-like $(NH_2Me_2)_{12}[(V_5O_9Cl)_6(NDC)_{12}]\cdot(DMF)_8(CH_3CH_2OH)_{0.5}$, $(NH_2Et_2)_8\{[V_6O_6(OCH_3)_9(SO_4)]_4(BDC)_6\}\cdot(DEF)_2$, and high nuclear polyoxoanion $[V^{V}{}_{17}V^{IV}{}_{12}(OH)_4O_{60}(OOC(CH_2)_4COO)_8]^{7-}$ [9–12].

Carboxylate covalently modified polyoxomolybdates are one of the most widely studied carboxylate functionalized POMs derivatives nowadays [7]. For example, the formate modified giant molecular cluster $[\{MoV_2O_4(HCOO)\}_{30}\{(Mo)Mo_5O_{21}(H_2O)_6\}_{12}]^{42-}$ (Mo_{132}) was reported in 1999 [13]. In 2002, Kortz *et al.* addressed a series of amino acid modified polyoxomolybdates $[XMo_6O_{21}(O_2CRNH_3)_3]^{n-}$ (n = 2, X = Se^{4+}, Te^{4+}; n = 3, X = As^{3+}, Sb^{3+}, B^{3+}; R = methylene, ethylene, cyclopropane, $CHCH_3$, $CH(CH_2)_4NH_2$) [14]. Since 2013, our group had launched the assembly system based heteropololymolybdate building units $[XMo_6O_{21}]^{n-}$ (X = HP^{3+}, As^{3+}, Sb^{3+}, Se^{4+}, Te^{4+}) with various aliphatic and aromatic carboxylate groups (from monocarboxylate, dicarboxylate to multicarboxylate), generating many carboxylate covalently modified heteropolymolybdates with abundant architectures featuring from monomer, dimeric, to hexameric clusters [15–19]. Among them, multiple examples of carboxylate covalently modified heteropolymolybdate displayed significant photochromic properties [16,18,19].

By comparison, the carboxylate covalently modified polyoxotungstates are relatively rare, mainly because the reaction activity between polyoxotungstates fragments and carboxylate

* Corresponding authors.
E-mail addresses: mpt@henu.edu.cn (P. Ma), jyniu@henu.edu.cn (J. Niu).

https://doi.org/10.1016/j.cclet.2022.02.043
1001-8417/

group is comparatively weak [7]. In this branch, Boskovic's group had made more contributions. They synthesized a series of carboxylate covalently modified arsenotungstates $[\{Ln(H_2O)_3\}_2\{As_2W_{19}O_{68}\}\{WO_2(L)\}_2]^{8-}$ (Ln = Y^{3+}, L = PdcH, Mcpc; Ln = Dy^{3+}, L = Pic), $[As_4(M_4)Mo^{VI}_xW^{VI}_{44-x}Y_4O_{160}(L)_y(H_2O)_z]^{n-}$ (M = combination of Mo, W and Y; L = Nle or Gly) and $[As_4(YW_3)W_{44}Y_4O_{159}(Gly)_8(H_2O)_{14}]^{9-}$ [20–23]. Li's group reported a tetrameric alanine modified arsenotungstate $[Ce_4As_4W_{44}O_{151}(ala)_4(OH)_2(H_2O)_{10}]^{12-}$ [24]. Our group had also prepared several examples of carboxylate covalently modified arsenotungstates such as hexameric cluster anion $\{Ln_2(H_2O)_4As_2W_{19}O_{68}(WO_2)_2(C_6O_7H_4)_2\}_3]^{33-}$ (Ln = Y^{3+}, Tb^{3+}, Dy^{3+}, Ho^{3+}, Er^{3+}, Tm^{3+}, Yb^{3+}, Lu^{3+}), and a one-dimensional (1D) chainlike POM $Na_4H_8[\{Pr(H_2O)_2\}_2\{As_2W_{19}O_{68}\}\{WO_2(mal)\}_2]\cdot 24H_2O$ (mal=malate) [25–27].

Recently, we launched the explorations on the system of the polyoxotungstates covalently modified by amino acid ligands. In this work, DL-serine (DL-Ser) ligand was chosen for the covalent modification with arsenotungstates based on the following considerations: (a) it as a chelating functional ligand with flexible amino and carboxyl coordination sites, which will result in the direction to form the larger high-nuclearity clusters by incorporating various metal centers such as La and W ions *via* multifunctional ligand patterns, implementing its organic functionalization; (b) it possesses amino and hydroxyl groups, significantly facilitating the establishment of rich intra- and/or inter-molecular hydrogen bonds in the targeted products between DL-Ser ligands and POMs skeleton, largely boosting the intra-molecular proton transition rate, thus becoming an ideal candidate for improving the opto-chemical and opto-physical properties of targeted products [8,28]. Fortunately, we successfully obtained a series of 1D linear chainlike DL-Ser covalently modified multinuclear Ln^{3+} implanted arsenotungstates $K_2[\{Ln(H_2O)_7\}_2\{As_4W_{44}O_{137}(OH)_{18}(H_2O)_2(DL\text{-}Ser)_2\}\{Ln_2(H_2O)_5(DL\text{-}Ser)\}_2]\cdot 65H_2O$ (Ln = La (**1**), Ce (**2**), Pr (**3**)), which all exhibited rapid photochromic behaviors.

X-ray crystal structure analyses indicated that compounds **1**–**3** are all isomorphic, which crystallized in triclinic *P*-1 space group (Table S1 in Supporting information). Therefore, only **1** was structurally descripted in detail. Bond valence sum (BVS) calculations of **1** indicated that the oxidation states of W, As, and La centers are +6, +3, and +3, respectively (Table S2 in Supporting information).

Structure analysis indicates that **1** is composed of 1D linear chainlike anion $[\{Ln(H_2O)_7\}_2\{As_4W_{44}O_{137}(OH)_{18}(H_2O)_2(DL\text{-}Ser)_2\}\{La_2(H_2O)_5(DL\text{-}Ser)\}_2]^{2-}$, two K^+ cations and 65 lattice water molecules. Specifically, this 1D framework is built up of the tetra-nuclear Ln^{3+} implanted DL-serine covalently modified arsenotungstate polyoxoanion $[\{As_4W_{44}O_{137}(OH)_{18}(H_2O)_2(DL\text{-}Ser)_2\}\{La_2(H_2O)_5(DL\text{-}Ser)\}_2]^{8-}$ (**1a**) (Fig. 1a). Regardless of the insertion of La^{3+} ions, the polyoxoanion **1a** can be considered as a double DL-Ser groups covalently modified arsenotungstate cluster $[As_4W_{44}O_{137}(OH)_{18}(H_2O)_2(DL\text{-}Ser)_2]^{18-}$, which consists of two distorted $\{As_2W_{19}O_{59}(OH)_8(H_2O)\}^{6-}$ building blocks linked together by a double DL-Ser ligands functionalized $[W_6O_{23}(OH)_2(DL\text{-}Ser)_2]^{14-}$ fragment (Fig. 1b). In the structure of **1a**, the $\{As_2W_{19}O_{59}(OH)_8(H_2O)\}^{6-}$ building blocks are distinctly different from the precursor $[As_2W_{19}O_{67}(H_2O)]^{14-}$ ($\{As_2W_{19}\}$) (Fig. S1 in Supporting information), and the opening angle in **1a** is obviously greater than that of the $\{As_2W_{19}\}$ precursor. This means that the $\{As_2W_{19}\}$ precursor undergo significant dissociation recombination or torsion deformation during the reaction process. Remarkably, the central part $\{WO_5(H_2O)\}$ group in $\{As_2W_{19}\}$ precursor changed from $\{WO_5(H_2O)\}$ to $\{WO_6\}$ in the assembly process of **1a**, also opening the As···W($\{WO_6\}$)···As angle. As a result, the As···As distance in **1** was 8.114(19) Å, which is obviously longer than the As···As distance in $\{As_2W_{19}\}$ precursor of 6.522(11) Å (Fig. S1), as well as the significantly larger angle

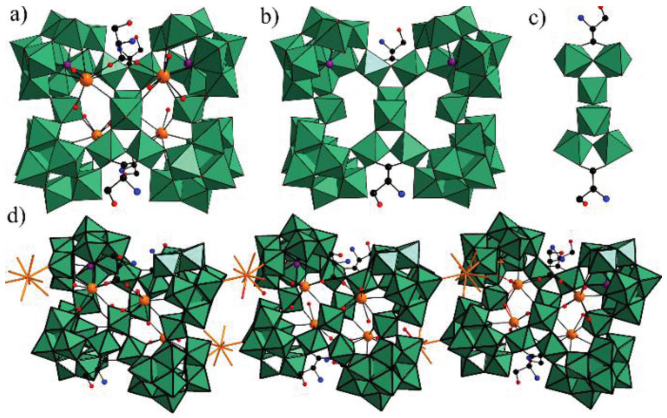

Fig. 1. (a) The polyhedron representation of the basic polyoxoanion unit in **1**: $[\{As_4W_{44}O_{137}(OH)_{18}(H_2O)_2(DL\text{-}Ser)_2\}\{La_2(H_2O)_5(DL\text{-}Ser)\}_2]^{8-}$. (b) The polyhedron representation of the polyoxoanion unit of $[As_4W_{44}O_{137}(OH)_{18}(H_2O)_2(DL\text{-}Ser)_2]^{18-}$. (c) The centrosymmetric Z-shaped hexatungstate $[W_6O_{23}(OH)_2(DL\text{-}Ser)_2]^{14-}$ fragment. (d) 1D linear chainlike polyoxoanion **1a** linked by peripheral La^{3+} ions.

As–W($\{WO_6\}$)–As(171.88(9)°) compared to the angle of 110.01(5)° in $\{As_2W_{19}\}$ precursor (Fig. S1), and this phenomenon has been reported before [28–30]. At the same time, the centrosymmetric Z-shaped $[W_6O_{23}(OH)_2(DL\text{-}Ser)_2]^{14-}$ segment (Fig. S2a) is made up of a pair of serine covalently modified $\{W_2O_9(DL\text{-}Ser)\}^{7-}$ groups, in which W1 and W2 (W3 and W4) atoms are connected by a chelating DL-Ser ligand and a μ_2–O atom, fused together by a corner-sharing $\{W_2O_5(OH)_2\}$ segment (Fig. 1c). Also, the $[W_6O_{23}(OH)_2(DL\text{-}Ser)_2]^{14-}$ segment is viewed as a pair of DL-serine covalently modified $\{W_3O_{11}(OH)(DL\text{-}Ser)\}^{6-}$ groups connected through a μ_2–O atom in the form of a common vertex μ_2–O atom from another perspective (Fig. S2b in Supporting information). Alternately, the polyoxoanion $[\{As_4W_{44}O_{137}(OH)_{18}(H_2O)_2(DL\text{-}Ser)_2\}\{La_2(H_2O)_5(DL\text{-}Ser)\}_2]^{8-}$ can also be viewed as a tetramer established by two [B-α-$AsW_9O_{29}(OH)_4]^{5-}$ subunits, two [B-α-$AsW_9O_{28}(OH)_4(H_2O)]^{3-}$ subunits, and a central $[\{W_8O_{43}(OH)_2(DL\text{-}Ser)_2\}\{La_2(H_2O)_5(DL\text{-}Ser)\}_2]^{32-}$ group (Fig. S3 in Supporting information). Moreover, **1a** is further stabilized by two embedded $[La_2(H_2O)_5(DL\text{-}Ser)]^{5+}$ groups, which is connected into 1D linear chainlike structure *via* two peripheral La^{3+} ions (Fig. 1d).

Moreover, the continuous-shape measure of three disparate La^{3+} ions are analyzed by SHAPE 2.1 software [31,32]. The eight-coordinate La1 exhibits a square antiprismatic (D_{4d}) geometry, while the La2 and La3 show a Muffin prism (C_s) of nine-coordinate and a spherical tricapped trigonal prism (D_{3h}) of nine-coordinate (Tables S3 and S4 in Supporting information), respectively. The coordination environment of La1, La2 and La3 in **1** are shown in Fig. S4 (Supporting information). Specifically, the La1 is defined by five μ_2–O atoms from five $\{WO_6\}$ octahedra, and two coordinated H_2O molecules, one O atom from DL-Ser ligand. The La2 is constructed from five μ_2–O atoms from five $\{WO_6\}$ octahedral, and three coordinated H_2O molecules, one O atom from DL-Ser ligand, while La3, as a linker, is defined by seven coordinated H_2O molecules, and two μ_2–O atoms from two $\{WO_6\}$ octahedra.

It is noteworthy that the multiple intra-molecular O–H···O and N–H···O hydrogen bonds interaction among DL-Ser ligands, POM skeleton and water molecules resides in the solid state structure of **1**. These detailed intra-molecular hydrogen bonds with the O–H···O and N–H···O distances in the range of 2.684(4)–3.216(5) Å are shown in Tables S5 and Fig. S5 (Supporting information), which further contributes to the stability of the crystal structure. More importantly, this will most likely facilitate electron transfer between DL-Ser ligands and POM components *via* hydrogen bonds pathway, improving the photochromic property of the matrix.

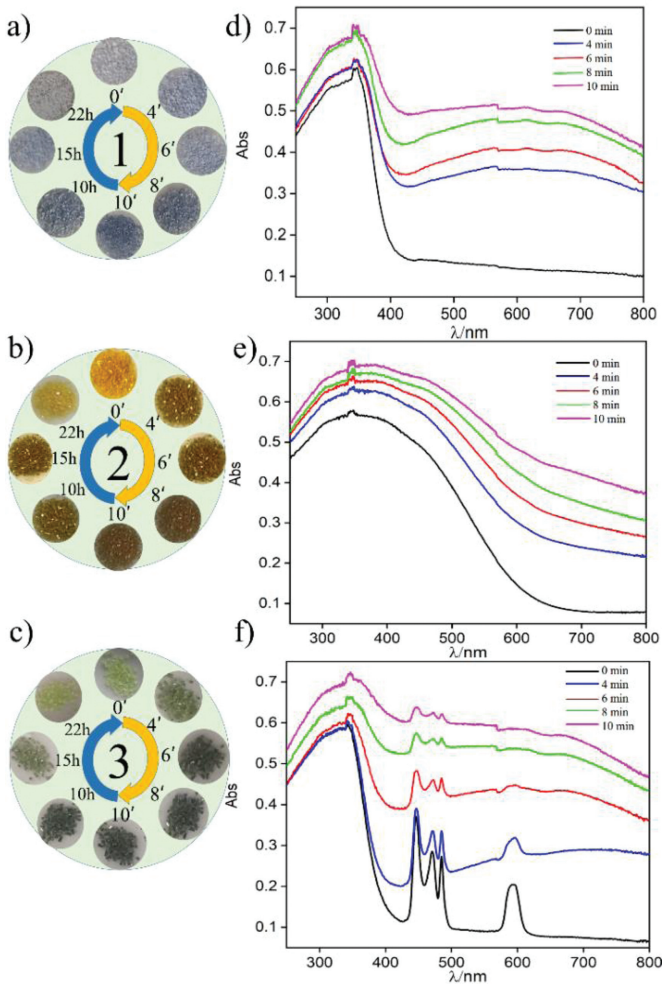

Fig. 2. (a–c) The color evolution for **1**–**3** irradiated after 0, 4, 6, 8, 10 min and the color fading in the dark under ambient conditions after 10 h, 15 h, 22 h. (d–f) The evolutions of the solid-state diffuse reflectance absorption spectra of **1**–**3** with irradiation times of 0, 4, 6, 8, 10 min.

Powder samples of **1**–**3** all exhibit rapid photochromic behaviors in response to UV irradiation. As shown in Figs. 2a–c, the crystalline state samples of **1**–**3** display white (**1**), yellow (**2**), green (**3**) color in the ground state, and which changed color to blue (**1**), brown (**2**) and glaucous (**3**) with the increment of the irradiation time. It apparently began to change color for about 4 min, and gradually reached saturation visible to the naked eye within 10 min. The IR spectra (Fig. S6 in Supporting information) and the PXRD patterns (Fig. S7 in Supporting information) of **1**–**3** before and after irradiation showed that all peak positions remained essentially unchanged, which further proved the stability of the structural skeleton. during the photochromic process. In addition, the irradiated samples were placed in the dark for about 22 h, which returned to their natural colors, thus suggesting that the **1**–**3** all display efficiently reversible photochromism.

In particular, the color changing of the first cycle was studied by UV-visible spectroscopy in the covered almost the entire visible spectrum, and the absorption spectra in 250–800 nm were collected under ambient conditions. There was no absorption band appears in the absorption spectra of **1** except for the UV absorption, attributing to the completely empty 4f orbital of La^{3+} with no f–f electron transition appeared. It was worth noting that a broad absorption band at around about 470 nm can be found in the UV-vis absorption spectra of **2**, which is due to the allowed 4f→5d electron transition of Ce^{3+} ions. The difference was that another four sharp absorption bands at about 447, 471, 487 and 593 nm in the UV-vis absorption spectra of **3**, which are ascribed to the f-f transitions $^3H_4 \rightarrow {}^3P_2$, $^3H_4 \rightarrow {}^3P_1$, $^3H_4 \rightarrow {}^3P_0$, $^3H_4 \rightarrow {}^7D_2$ of Pr^{3+} ions. Most importantly, the obvious broad bands in the range of 500–800 nm about centered at 675 nm for **1**, 575 nm for **2** and 673 nm for **3** are observed in their absorption spectra when increasing irradiation times, which is obviously ascribed to the occurrence of electron-transfer process as a result of the metal-to-metal extra inter-valence charge-transfer inter valence charge transfer (IVCT) $W^{VI} \rightarrow W^{V}$ (Figs. 2d–f) [7,23].

In addition, we investigated the solid-state photochromic properties of **1**–**3**. The diffuse reflectance spectra of **1**–**3** were performed in the range of 250–800 nm, and the reflectance values of Kubelka-Munk (K–M) functions were also calculated [31]. The diffuse reflectance spectra of samples **1**–**3** and their associated K–M transform plots can be seen that the optical gaps of **1**–**3** before radiation were 3.07 eV, 2.05 eV and 3.11 eV, respectively. Then, by calculating the optical gap of **1**–**3** under a certain period of irradiation, the optical gaps significantly decreased to 2.13 eV, 1.37 eV and 1.45 eV, respectively, manifesting that the photochromic reaction triggered after irradiation (Fig. S8 in Supporting information). The absorption change of intensity at broad bands visible region under irradiation and recovery is shown in Fig. S9 (Supporting information), the absorption intensity at ~675 nm for **1**, ~575 nm for **2** and ~673 nm for **3** could maintain about 93.2%, 90.3% and 92.5% of their first values after six cycles, which demonstrate excellent reversible photochromic behavior of **1**–**3** with a repeatability of no less than 6 cycles.

Considering above-mentioned abundant hydrogen bonding in solid state structures of **1**–**3**, it can be inferred that the photochromic mechanism of **1**–**3** relies on Yamase's model for the charge transfer (CT) aspect of the photochromic mechanism [33,34]. Therefore, similar to the mechanism proposed by Yamase's group, the electron transfer occurs between the terminal oxygen atom of the POM cluster and its connecting W^{VI} atom, induced by the multiple intra-molecular O–H···O and N–H···O hydrogen bonding pathway between the DL-serine ligand and POM components under high-power irradiation (Scheme 1).

Additionally, we carried out the study of the kinetics of the coloration of **1**–**3**. According to the theory proposed by Desssapt's group, the coloration rate is related to the concentration of inducible W^{VI} center with irradiation time and follows a second-order reaction law [35–38]. The reflectance values of **1**–**3** at the wavelength of maximum absorbance versus irradiation time in the range of 250–800 nm were shown in Fig. 3. It can be seen that the light values abruptly decreased and then tended to a slight flatten with the duration of irradiation. The curves of reflectivity $R(t)$ *vs.* t for **1**–**3** can be well-fitted using the function [31,39,40]:

$$R_{max}(t) = a/(bt+1) + R_{max}(N) = a/(bt+1) + c \quad (1)$$

a and b: proportional constants, $c = R_{max}(N)$. The photochromic rate (half-life), $t_{1/2}$, is the time required to reach $[R(0)+R(N)]/2$, approximately $t_{1/2} = 1/b$. The relative parameters can be obtained by the curve fitting and listed in Fig. 3. The $t_{1/2}$ values from the curve

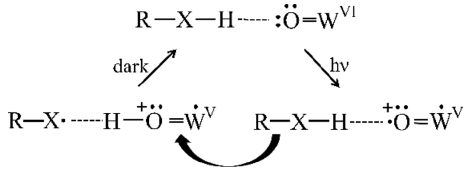

Scheme 1. The photochromic mechanism of **1**–**3**. X represents N or O atoms in the serine ligand.

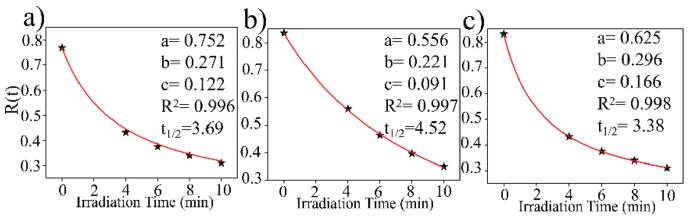

Fig. 3. The plots of reflectivity $R(t)$ *vs.* t for **1** (a) **2** (b) and **3** (c) measured at 675 nm, 575 nm, 673 nm for 0, 4, 6, 8 and 10 min irradiation.

fitting were 3.69 min, 4.52 min and 3.38 min. The coloration speeds of **1**–**3** are all evidently fast, which are comparable with most fast photochromic polyoxotungstates (Table S6 in Supporting information). In addition, the rapid photochromic behavior is closely related to the low optical band gaps and rich intramolecular hydrogen bonds of **1**–**3** during the photochromism [41].

In summary, a series of isostructural 1D linear chainlike DL-Ser ligands covalently modified multinuclear lanthanide implanted arsenotungstates: $K_2[\{Ln(H_2O)_7\}_2\{As_4W_{44}O_{137}(OH)_{18}(H_2O)_2$(DL-Ser)$_2\}\{Ln_2(H_2O)_5$ (DL-Ser)$\}_2]\cdot 65H_2O$ (DL-Ser = DL-serine, Ln = La (**1**), Ce (**2**), Pr (**3**)), were successfully obtained by reaction of $K_{14}[As_2W_{19}O_{67}(H_2O)]$ precursor and DL-Ser ligands through a facile aqueous solution assembly. The 1D framework is established by using the DL-serine ligand covalently modified tetra-nuclear Ln^{3+} ions implanted arsenotungstate polyoxoanion $[\{As_4W_{44}O_{137}(OH)_{18}(H_2O)_2$(DL-Ser)$_2\}\{La_2(H_2O)_5$(DL-Ser)$\}_2]^{8-}$, which is constituted of two $\{As_2W_{19}O_{59}(OH)_8(H_2O)\}^{6-}$ subunits, a core $[W_6O_{23}(OH)_2$(DL-Ser)$_2]^{14-}$ segment and two implanted $[Ln_2(H_2O)_5$(DL-Ser)$]^{5+}$ groups. Additionally, **1**–**3** display excellent photochromic behaviors in response to UV irradiation. Moreover, the hydrogen bond interaction between POM components and DL-Ser ligands greatly improves the photochromic properties of these compounds. This not only enrich the field of POMs chemistry, but pave the way towards understanding the POMs-based photochromic materials.

Declaration of competing interest

The authors declare that they have no known competing financial interests or personal relationships that could have appeared to influence the work reported in this paper.

Acknowledgments

This work was supported by the National Natural Science Foundation of China (No. 222071043), the Major Project of Science and Technology, Education Department of Henan Province (No. 20A150010) and the 2021 Students Innovative Pilot Plan of Henan University (No. 202110475079).

Supplementary materials

Supplementary material associated with this article can be found, in the online version, at doi:10.1016/j.cclet.2022.02.043.

References

[1] H.G. He, G.W. Wang, S.C. Chai, et al., Chin. Chem. Lett. 32 (2021) 2013–2016.
[2] L. Cronin, A. Muller, Chem. Soc. Rev. 41 (2012) 7333–7334.
[3] T.P. Hu, Zhao Y.Q, Z. Jagličić, et al., Inorg. Chem. 54 (2015) 7415–7423.
[4] Y.Q. Zhao, K. Yu, L.W. Wang, et al., Inorg. Chem. 53 (2014) 11046–11050.
[5] J.J. Walsh, A.M. Bond, R.J. Forster, T.E. Keyes, Coord. Chem. Rev. 306 (2016) 217–234.
[6] G.P. Yang, Y. Liu, K. Li, et al., Chin. Chem. Lett. 31 (2020) 3233–3236.
[7] P.T. Ma, H Feng, J.P. Wang, J.Y. Niu, Coord. Chem. Rev. 378 (2019) 281–309.
[8] P.T. Ma, H Feng, R. Wan, et al., J. Mater. Chem. C 4 (2016) 5424–5433.
[9] Y.T. Zhang, X.L. Wang, S.B. Li, et al., Inorg. Chem. 55 (2016) 8770–8775.
[10] Y.T. Zhang, X.L. Wang, S.B. Li, et al., Chem. Commun. 52 (2016) 9632–9635.
[11] Y.T. Zhang, S.B. Li, X.L. Wang, et al., Dalton Trans. 45 (2016) 14898–14901.
[12] K. Wang, N.J. Niu, D.Y. Zhao, et al., Inorg. Chem. 56 (2017) 14053–14059.
[13] A. Muller, V.P. Fedin, C. Kuhlmann, H. Bogge, M. Schmidtmann, Chem. Commun. (1999) 927–929.
[14] U. Kortz, M.G. Savelieff, F.Y.A. Ghali, et al., Angew. Chem. Int. Ed. 41 (2002) 4070–4073.
[15] D.H. Yang, Y.F. Liang, P.T. Ma, et al., CrystEngComm 16 (2014) 8041–8046.
[16] Y.F. Liang, S.Z. Li, D.H. Yang, et al., J. Mater. Chem. C 3 (2015) 4632–4639.
[17] D.H. Yang, S.Z. Li, P.T. Ma, J.P. Wang, J.Y. Niu, Inorg. Chem. 52 (2013) 14034–14039.
[18] D.H. Yang, Y.F. Liang, P.T. Ma, et al., Inorg. Chem. 53 (2014) 3048–3053.
[19] D.H. Yang, S.Z. Li, P.T. Ma, J.P. Wang, J.Y. Niu, Inorg. Chem. 52 (2013) 8987–8992.
[20] M.R. Healey, R.W. Gable, C. Ritchie, C. Boskovic, Polyhedron 64 (2013) 13–19.
[21] C. Ritchie, C.E. Miller, C. Boskovic, Dalton Trans. 40 (2011) 12037–12039.
[22] M. Vonci, F.A. Bagherjeri, P.D. Hall, et al., Chem. Eur. J. 20 (2014) 14102–14111.
[23] F.A. Bagherjeri, M. Vonci, E.A. Nagul, et al., Inorg. Chem. 55 (2016) 12329–12347.
[24] X.J. Feng, H.Y. Han, Y.H. Wang, et al., CrystEngComm 15 (2013) 7267–7273.
[25] P.T. Ma, R. Wan, Y.N. Si, et al., Dalton Trans. 44 (2015) 11514–11523.
[26] Y. Wang, X.P. Sun, S.Z. Li, et al., Cryst. Growth Des. 15 (2015) 2057–2063.
[27] J. Wang, W.J. Shi, S.J. Li, et al., Dalton Trans. 47 (2018) 7949–7955.
[28] H.L. Li, Y.J. Liu, J.L. Liu, et al., Chem. Eur. J. 23 (2017) 2673–2689.
[29] C. Ritchie, M. Speldrich, R.W. Gable, L. Sorace, C. Boskovic, Inorg. Chem. 50 (2011) 7004–7014.
[30] H.C. Wu, R. Wan, Y.N. Si, et al., Dalton Trans. 47 (2018) 1958–1965.
[31] B. Yan, H.C. Wu, P.T. Ma, J.P. Wang, J.Y. Niu, Inorg. Chem. Front. 8 (2021) 4158–4176.
[32] B. Yan, R.C. Liang, K.T. Zheng, et al., Inorg. Chem. 60 (2021) 8164–8172.
[33] T. Yamase, Chem. Rev. 98 (1998) 307–326.
[34] T. Yamase, M. Sugeta, J. Chem. Soc. Dalton Trans. (1993) 759–765.
[35] E. Papaconstantinou, Chem. Soc. Rev. 18 (1989) 1–31.
[36] R. Dessapt, M. Collet, V. Coue´, et al., Inorg. Chem. 48 (2009) 574–580.
[37] O. Oms, T. Benali, J. Marrot, et al., Inorganics 3 (2015) 279–294.
[38] R.C. Howell, F.G. Perez, S. Jain, et al., Angew. Chem. Int. Ed. 40 (2001) 4031–4034.
[39] J. Wang, P.T. Ma, Y.P. Wang, et al., J. Phys. Chem. Solids. 110 (2017) 161–166.
[40] V. Coué, R. Dessapt, M. Bujoli-Doeuff, M. Evain, S. Jobic, Inorg. Chem. 46 (2007) 2824–2835.
[41] Y.F. Liang, S.Z. Li, D.H. Yang, et al., J. Mater. Chem. C 3 (2015) 4632–4639.